CHEMISTRY
A EUROPEAN JOURNAL

Supporting Information

The EXAFS analysis of bulk and supported vanadium oxide species

Daphne E. Keller[a], Bert M. Weckhuysen*,[a] and Diek C. Koningsberger*[a]

A1.1 Results of the EXAFS analysis and other spectroscopic techniques

XAFS spectroscopy of Na_3VO_4 and V_2O_5

The structures of Na_3VO_4 and V_2O_5 are well known from XRD data. Their structural parameters are listed in Table A1. The XANES spectra of Na_3VO_4 and V_2O_5 are displayed in Figure A1. It can be seen that pre-edge peak of Na_3VO_4 (tetrahedron) is much more intense than for V_2O_5 (square pyramid). When the vanadium oxide cluster has an inversion centre, as in an regular octahedral environment, the 1s -> 3d transition is strictly dipole forbidden resulting in the absence of the pre-edge peak. Lowering the symmetry of the ligands and breaking the inversion centre, however, causes the pre-edge absorption to become dipole allowed. Wong *et al.* have shown that the intensity should be between 0.8 and 1 for a perfect tetrahedron.[39] The value observed for Na_3VO_4 is indeed 1, typical for a regular tetrahedron. The value observed for V_2O_5 is 0.65, implying that indeed the coordination geometry moves away from tetrahedron symmetry to square pyramidal.

The FT's (k^1, Δk = 2.5 – 10 $Å^{-1}$) of the raw EXAFS data are shown in Figure 2 (solid lines). Multiple shell fitting in R-space was applied to determine the different absorber-back-scatterer pairs contributing to the FT between 0.8 < R < 1.5 Å for Na_3VO_4 and 0.7 < R < 2.2 Å for V_2O_5. All contributions were fitted at the same time in R-space with simultaneously inspection of the FT of the difference file and calculated fit of each individual contribution. The Fourier transforms of the final fit are presented in Figure 2 (dashed lines). The crystallographic coordination numbers and inter-atomic distances are used as input parameters for the fit. The deviation in the low regions of R (R < 0.5 Å) is due to the AXAFS contribution of the spectrum that is not incorporated in the fit. Variations between the raw and experimental data at higher values of R are caused by the contributions of higher shells to the spectrum that were not incorporated in the fit. The parameters obtained from the fits are listed in Tables A2 and A3. The variances of the absolute and imaginary part are acceptable. The number of independent free parameters (N_{free}) calculated according to the Nyquist theorem[40] for the fit of the Na_3VO_4 data amounts 5.3 and for the fit of the V_2O_5 data 8.7. This indicates that the fit of Na_3VO_4 is statistically allowed, since the number of parameters used for the R-space fit is 2. Whereas the fit of V_2O_5 slightly exceeds the allowed number of parameters.

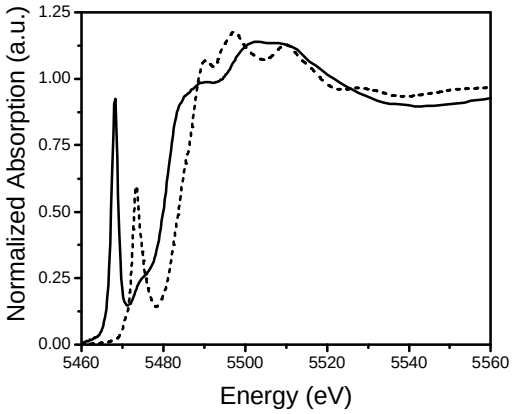

Figure A1: The pre-edge and XANES region of the XAFS spectra of samples Na_3VO_4 (—) and V_2O_5 (---), measured at 77 K.

Table A1: Crystallographic parameters for reference compounds

	bond type and distances (Å)*								
	V=O	V-O						V---O	ref
Na_3VO_4		1.696 (4x)							41
V_2O_5	1.58	1.779	1.878 (2x)	2.017				2.79	42,43
V_4O_7[a]		1.883	1.897	1.937	2.032	2.042	2.101		39
V_2O_3		1.96 (3x)	2.06 (3x)						39

*Coordination between brackets; [a] average V-O distance is 1.98 Å.

Table A2: Structural parameters for the total fit in k^2 weighting of bulk Na_3VO_4. Dk = 2.5 – 10 $Å^{-1}$; DR = 0.80 – 1.70 Å.

					Variances (%)	
	N*	R (Å)*	$\Delta\sigma^{2*}$	ΔE_0 (eV)*	Im	Abs
$V\text{-}O_{(1)}$	4^+	1.70^+	-0.00039	1.69	0.4	0.3

* N = coordination number; R = distance in Å; $\Delta\sigma^2$ = Debye-Waller factor, i.e. disorder; E_0 = inner potential (eV). + fixed input parameters

Table A3: Structural parameters for the total fit in k^2 weighting of bulk V_2O_5. Dk = 2.5 – 10 $Å^{-1}$; DR = 0.80 – 2.20 Å.

					Variances (%)	
	N*	R (Å)*	$\Delta\sigma^{2*}$	ΔE_0 (eV)*	Im	Abs
$V{=}O_{(1)}$	1^+	1.58^+	0.00090	6.74	7.2	1.9
$V\text{-}O_{(2)}$	1^+	1.779^+	0.00289	3.85		
$V\text{-}O_{(3)}$	2^+	1.878^+	0.00005	4.28		
$V\text{-}O_{(4)}$	1^+	2.017^+	0.02000	1.36		

V---$O_{(5)}$	1^{+}	2.790^{+}	0.02000	6.46

* N = coordination number; R = distance in Å; $\Delta\sigma^2$ = Debye-Waller factor, i.e. disorder; E_0 = inner potential (eV). + fixed input parameters

Raman, UV-VIS, ESR of 1V-Al-D and 1V-Al-R

The Raman spectra of the dehydrated and the hydrogen treated 1 wt% catalyst are presented in Figure A2A. The spectra are characterised by a sharp peak at 1023 cm^{-1}, assigned to the V=O stretch vibration in an isolated VO_4 species, and a broad band at ~900 cm^{-1}, which is indicative of the presence of monomeric species as well.[32,44,45] Altogether, all the characteristics of the Raman spectrum of 1V-Al-D are still present in the spectrum of 1V-Al-R, suggesting that the vanadium oxide species were only partially reduced. The UV-VIS DRS spectra of 1V-Al-D and 1V-Al-R are shown in Figure A2B. The spectra are dominated by the large charge transfer (CT) transition above 3.8 eV. D-d transitions are not observed for the 1V-Al-D. The absence of V^{4+} in the 1V-Al-D sample, as indicated by the UV-VIS DRS measurement, was further checked with ESR measurements. The ESR data showed no significant amount of vanadium (IV) present in this sample (< 1%). The hydrogen treated sample (1V-Al-R), however, does show some d-d transitions in the UV-VIS spectrum indicating that the electron density on the vanadium atom is increased. This was supported by ESR, that showed paramagnetic activity of the vanadium clusters. So, UV-VIS and ESR suggest at least a partial reduction of the vanadium oxide species.

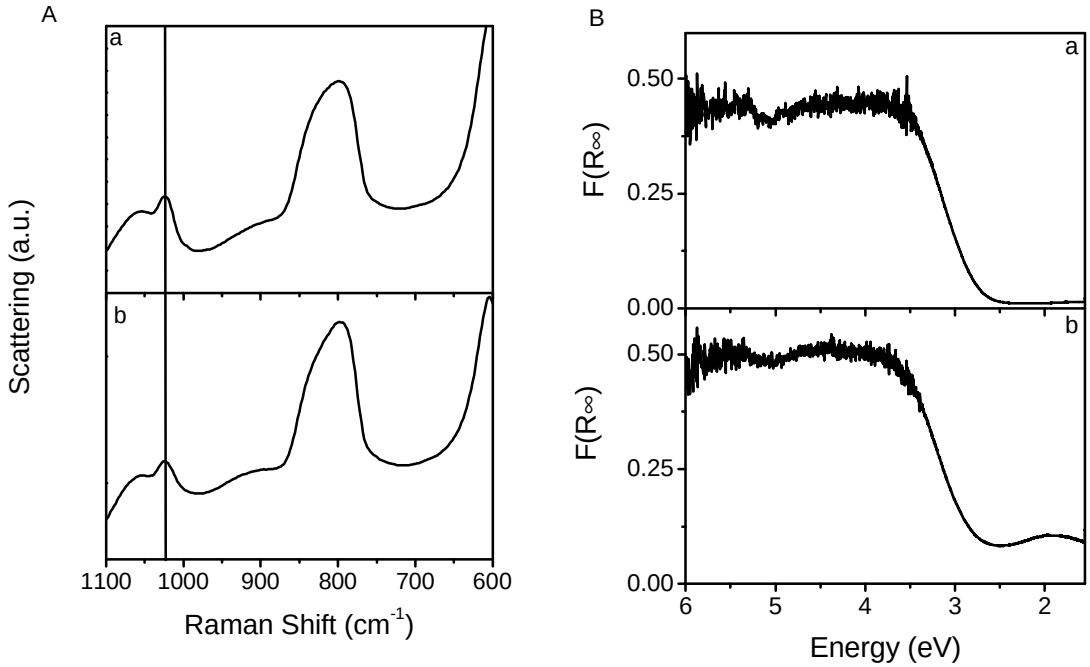

Figure A2: (A) Raman spectra of 1V-Al obtained at room temperature. (a) after dehydration pre-treatment; (b) after reduction pre-treatment. (B) UV-VIS DRS spectra of 1V-Al obtained at room temperature. (a) after dehydration pre-treatment; (b) after reduction pre-treatment.

XAFS spectroscopy of 1V-Al-D and 1V-Al-R

Figure A3 shows the XANES spectra of 1V-Al-D (solid line) and 1V-Al-R (dashed line). It can be seen that the pre-edge intensity of the de-hydrated sample amounts 0.66, while the pre-edge intensity of the reduced sample is 0.38. The value of 1V-Al-D is too low for a perfect tetrahedron. This value implies the absence of an inversion centre and a distortion from a perfect tetrahedron (e.g. C_{3v}). The pre-edge intensity of 1V-Al-R is too low for a perfect tetrahedron and too high for a regular octahedron, but it resembles the value obtained for bulk V_2O_4.[39] The distance between the pre-edge peak and the edge is a measure for the oxidation state and an indication of the coordination of vanadium in the sample.[39] For the 1V-Al-D sample a value of 12.5 eV was observed, while the difference is 12.0 eV for the 1V-Al-R sample. Literature values for tetrahedral V(V) species lie between 12.4 and 13.5 eV. For a square pyramidal V(V) in V_2O_5 the E_{edge}-$E_{pre\text{-}edge}$ value is 9.5 eV.[39] Using these literature data one can conclude that vanadium is 5+ and fourfold coordinated in 1V-Al-D. A lower oxidation state of vanadium leads to a lower E_{edge}-$E_{pre\text{-}edge}$ value. This is illustrated by distorted octahedrons V_2O_3 (V(III)) with a value of 7.3 eV and V_2O_4 (V(IV)) with a value of 9.5 eV. It has to be mentioned that also higher values can be observed for a distorted square pyramid like VOPBD (vanadyl bis(1-phenyl-1,3-butane)dionate), which has a value of 10.8 eV. However, since all reference compounds with vanadium valence states lower than 5+ have values lower 9.5 eV, one has to conclude that that the extend of reduction in 1V-Al-R is not very high.

Based on the results of all characterization techniques presented above we tentatively assume that only part of the vanadium oxide clusters in 1V-Al-R are reduced. This would imply that a mixture of the original dehydrated fourfold coordinated vanadium and reduced octahedrally coordinated vanadium is present in the hydrogen treated vanadium oxide catalyst.

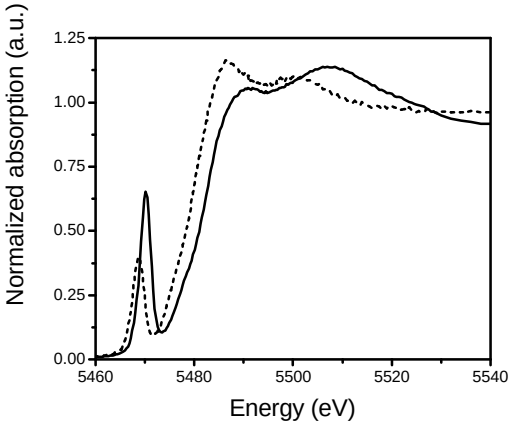

Figure A3: XANES region of the XAFS spectrum for 1V-Al-D (—) and 1V-Al-R (---), with a clear pre-edge peaks, measured at 77 K.

The EXAFS spectra obtained after background subtraction, using the procedure as illustrated above, and normalization are shown in Figure A4a. The signal to noise ratio is 53 for the 1V-Al-D and 47 for 1V-Al-R, with the amplitude determined between k = 2.5 and 4 Å-1 and the noise level between k = 11 and 13 Å-1. The difference in the raw EXAFS data is obvious, indicating a change in vanadium oxide structure upon reduction in hydrogen. This can clearly be seen in the corresponding Fourier transforms (k1, Δk = 2.5 – 11 Å-1), which are plotted in Figure A4b.

The data could be fit with a monomeric VO4 species with one V=O bond, two V-O bonds and one V-O(b)-Msupport bond. An overview of the fit results is presented in Table A4 and Figure 4 for comparison. The fit of the EXAFS data of the 1V-Al-R sample was based upon the assumption that a mixture of two different vanadium compound is present in the reduced sample. The best fit was obtained with a mixture of 70% dehydrated VO4 and 30% reduced vanadium species. The reduced species resembled the octahedrally coordinated V_4O_7, with six oxygen neighbours at an average distance of 1.98 Å. It has to be mentioned that the R-space fit was carried only within the range 0.7 < R < 2.0 Å describing the first shell tetrahedron and octahedron contributions. It was not possible to include in the fit any higher shell interfacial contributions, since two different oxide species are present each having their own interfacial structure. The number of independent free parameters allowed for the fit amounted to nine. Three coordination shells were fitted (tetrahedral: 2, octahedral: 1).

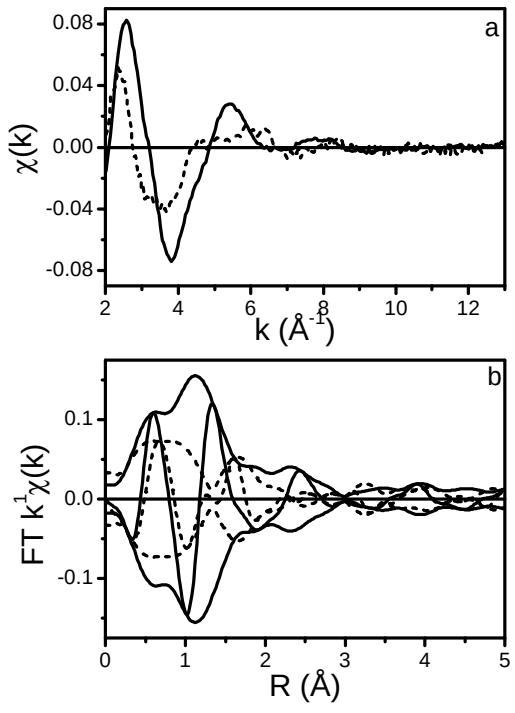

Figure A4: (a) Experimental EXAFS data (χ(k)) of 1V-Al-D (—) and 1V-Al-R (---), measured at 77 K. (b) k^1 weighted Fourier Transform of the experimental χ(k) for 1V-Al-D (—) and 1V-Al-R (---).

Table A4: Structural parameters for the total fit of 1V-Al-D for the total fit in k^1 weighting. (Dk = 2.5-11 Å^{-1}, DR = 0.7-5.0 Å)

					Variances (%)	
	N*	R (Å)*	$\Delta\sigma^{2*}$	ΔE_0 (eV)*	Im	Abs
V=$O_{(1)}$	1+	1.58+	-0.0003	13.6	0.8	0.7
V-$O_{(2)}$	3+	1.72	0.00772	3.1		
V---$O_{(3)}$	1+	2.29	0.0133	-4.4		
V---$Al_{(4)}$	1+	3.09	0.015	6.8		
V---$O_{(5)}$	2+	3.50	0.008	-3.1		
V---$O_{(6)}$	2+	4.32	0.012	3.1		

* N = coordination number; R = distance in Å; $\Delta\sigma^2$ = Debye-Waller factor, i.e. disorder; E_0 = inner potential (eV). + fixed input parameters

The coordination distances of the tetrahedron VO_4 are known, the ratio tetrahedral/octahedral is used as input parameter as well. The number of free parameters needed for the fit is therefore eight, implying that the fit is statistically allowed. The parameters for the best fit are listed in Table A5. The total fit for the 1V-Al-R is presented in Figure 4b (dashed line). The deviations at low values of R (R < 0.5 Å) are due to the AXAFS contribution. The presence of higher shell contributions are causing the differences at values for R > 2 Å. The presence of a V_4O_7 type species can indeed explain the decrease in the pre-edge intensity, the edge position, the d-d transitions in the UV-VIS DRS spectrum and the observed ESR signal.

XAFS spectroscopy of 5V-Al-D, 10V-Al-D and 20V-Al-D

The XANES spectra as a function of the vanadium loading are plotted in Figure A5. It can be seen that 5V-Al-D has the highest intensity between 5480 < E < 5500 eV. However, the intensity of the pre-edge peak for this sample is the lowest and increases in the order of increasing vanadium loading, implying an increasing degree of tetrahedral symmetry around the vanadium absorber.

The Fourier transforms of the raw EXAFS data are presented in Figure A6. Large differences can be observed between 5V-Al-D and the other two samples for values of R between 0.5 and 1.8 Å. Especially the nodes in the imaginary part around 1.65 Å are remarkably different for 5V-Al-D. The FT region, where also V---V interactions are expected (2.5 < R < 3 Å) is different for all samples.

Table A5: Structural parameters for the total fit in k^1 weighting of 1V-Al-R, with 70% of the oxidised VO_4 species and 30% reduced species (octahedral). Dk = 2.5 – 11 $Å^{-1}$; DR = 0.7 – 2 Å.

					Variances (%)	
	N*	R (Å)*	$\Delta\sigma^{2*}$	ΔE_0 (eV)*	Im	Abs
$V{=}O_{(1)}$	0.67+	1.58+	-0.00205	9.86	4	3
$V\text{-}O_{(2)}$	2.11+	1.71	0.00897	7.18		
$V\text{-}O_{(3)}$	1.87+	1.98	-0.00006	6.10		

* N = coordination number; R = distance in Å; $\Delta\sigma^2$ = Debye-Waller factor, i.e. disorder; E_0 = inner potential (eV). + fixed input parameters

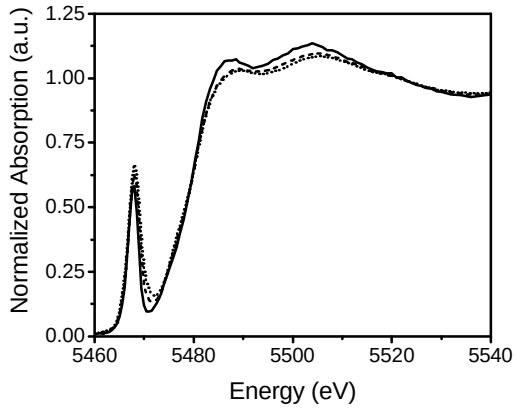

Figure A5: XANES region of the XAFS spectrum for 5V-Al (—), 10V-Al (---) and 20V-Al (···), with a clear pre-edge peaks, measured at 77 K.

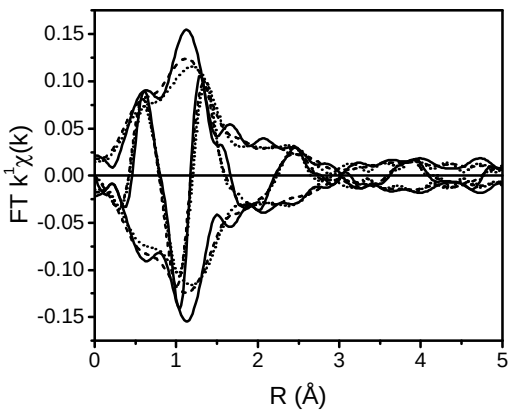

Figure A6: k^1 weighted Fourier Transforms of the experimental $\chi(k)$ of 5V-Al(—), 10V-Al (---) and 20V-Al (···).

Multiple shell fitting in R-space was applied with in combination with a structural model obtained with the Cerius[2] software. During the fitting process it became clear that the basic structure of all samples consists of VO_4 units. In 5V-Al-D the VO_4 unit is surrounded by other isolated VO_4 units at an average V---V distance of about 3.5 Å. With increasing vanadium loading chemical bonds are formed between the different VO_4 units resulting in a shorter average V---V distance of about 2.95 Å. Higher vanadium loading also leads to a higher V---V coordination number up to a maximum of 2 for 20V-Al-D. The FT's (k^1, $\Delta k = 2.5 - 11$ $Å^{-1}$) of the raw EXAFS data and the fits are displayed in Figure 5. The resulting EXAFS coordination parameters are given in Tables A6-A8. The interactive approach of R-space fitting with the use of a structural model from Cerius[2] made it possible to incorporate not only higher coordination shells arising from scatters in the interface with the supporting oxide, but also from nearby VO_4 units. The remarkable differences in the higher coordination shells as a function of increasing vanadium loading can be illustrated by plotting the FT of the difference files [raw EXAFS minus ($V\text{-}O_{(1)}$ + $V\text{-}O_{(2)}$)] and the FT of the corresponding sum of the higher coordination shells (see Figure A7).

Table A6: Structural parameters for the total fit of 5V-Al. Dk = 2.5 – 11 $Å^{-1}$; DR = 0.7 – 4 Å.

					Variances (%)	
	N*	R (Å)*	$\Delta\sigma^{2*}$	ΔE_0 (eV)*	Im	Abs
$V{=}O_{(1)}$	0.96+	1.58+	-0.0003	13.04	3	1
$V\text{-}O_{(2)}$	3.02+	1.72+	0.00908	3.73		
$V\text{---}O_{(3)}$	1.03+	2.10	0.00050	-2.31		
$V\text{---}O_{(4)}$	1.00+	2.36	0.00608	-3.06		
$V\text{---}Al_{(5)}$	0.93+	3.07	0.00618	2.99		
$V\text{---}V_{(6)}$	1.07	3.50	0.00870	5.06		
$V\text{---}O_{(7)}$	0.97+	2.91	0.00500	14.90		

* N = coordination number; R = distance in Å; $\Delta\sigma^2$ = Debye-Waller factor, i.e. disorder; E_0 = inner potential (eV). + fixed input parameters

Table A7: Structural parameters for the total fit of 10V-Al. Dk = 2.5 – 11 $Å^{-1}$; DR = 0.7 – 4 Å.

					Variances (%)	

	N*	R (Å)*	$\Delta\sigma^{2*}$	ΔE_0 (eV)*	Im	Abs
$V{=}O_{(1)}$	0.96+	1.58+	-0.00320	-4.17	1	1
$V{-}O_{(2)}$	3.02+	1.72+	0.00210	7.98		
$V{---}O_{(3)}$	1.05+	2.70	0.000625	-12.87		
$V{---}Al_{(4)}$	0.95+	3.16	0.01322	7.71		
$V{---}V_{(5)}$	1.16	2.95	0.02500	-6.84		
$V{---}O_{(6)}$	0.99+	3.20	0.02154	6.23		
$V{---}O_{(7)}$	2.38+	3.45	0.00424	14.18		

* N = coordination number; R = distance in Å; $\Delta\sigma^2$ = Debye-Waller factor, i.e. disorder; E_0 = inner potential (eV). + fixed input parameters

Table A8: Structural parameters for the total fit of 20V-Al. Dk = 2.5 – 11 Å^{-1}; DR = 0.7 – 4 Å.

					Variances (%)	
	N*	R (Å)*	$\Delta\sigma^{2*}$	ΔE_0 (eV)*	Im	Abs
$V{=}O_{(1)}$	0.96+	1.58+	-0.00350	-3.18	1	0.6
$V{-}O_{(2)}$	3.01+	1.71+	0.00065	10.81		
$V{---}O_{(3)}$	1.11+	2.67	0.00872	-12.29		
$V{---}Al_{(4)}$	0.95+	3.16	0.02000	8.27		
$V{---}V_{(5)}$	2.05	2.95	0.02565	-5.92		
$V{---}O_{(6)}$	0.99+	3.20	0.00292	4.35		
$V{---}O_{(7)}$	4.08+	3.56	0.02200	9.48		

* N = coordination number; R = distance in Å; $\Delta\sigma^2$ = Debye-Waller factor, i.e. disorder; E_0 = inner potential (eV). + fixed input parameters

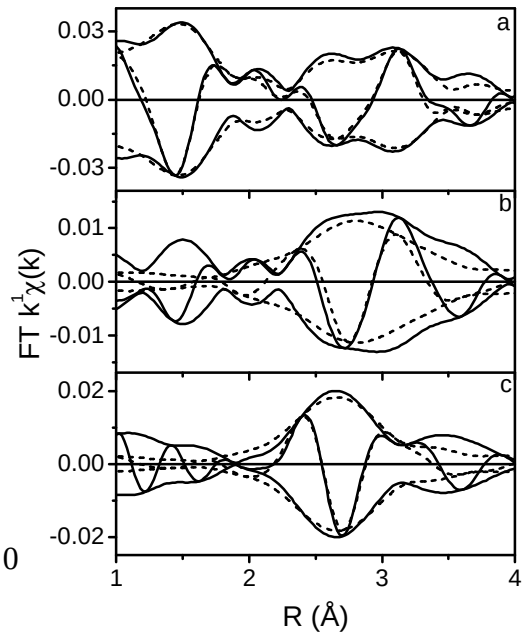

Figure A7: k^1 weighted Fourier Transforms of difference files (Raw-$O_{(1)}$-$O_{(2)}$) (—) together with the sum of the higher shells (---). (a) 5V-Al ($O_{(3)}$+$O_{(4)}$+$Al_{(5)}$+$V_{(6)}$+$O_{(7)}$), (b) 10V-Al ($O_{(3)}$+$Al_{(4)}$+$V_{(5)}$+$O_{(6)}$+$O_{(7)}$) and 20V-Al ($O_{(3)}$+$Al_{(4)}$+$V_{(5)}$+$O_{(6)}$+$O_{(7)}$).

A.1.2 Discussion on the EXAFS analysis

Influence of reduction on the structure of 1V-Al-D

The clear presence of the V=O vibration at ~1020 cm^{-1} in the reduced 1V-Al sample, suggests that the vanadium oxide species in the catalyst are not entirely reduced in the hydrogen treatment. This idea is supported by the relatively small decrease in the pre-edge intensity in the XANES spectrum upon reduction. For a total reduction from 5+ to 3+/4+ a much larger decrease is expected, on the basis of bulk reference compounds.[39] However, ESR and UV-VIS measurements indicated that reduction of the vanadium species took place to some extend. The UV-VIS spectrum showed some intensity in the d-d transition region of the spectrum and the ESR spectrum showed paramagnetic V^{4+} species were present in the sample. Trivalent and tetravalent vanadium species occur mainly in 5-fold or 6-fold coordination and the decrease in pre-edge intensity implies a change in coordination toward a more centro-symmetric structure: 5 or 6 coordinated.[46,47]

Combining the information from Raman, XANES, UV-VIS and ESR, the EXAFS data were fit with a mixture of two species: the monomeric VO_4 species in 5+ oxidation state (70%) and an octahedrally coordinated reduced species, resembling V_4O_7 (30%). This resulted in a good fit, indicating that the reduced 1V-Al catalysts contained V^{5+} tetrahedral monomers together with V^{3+}/V^{4+} octahedrally coordinated species.

Structure of 5V-Al-D, 10V-Al-D and 20-Al-D

The higher shells observed in the FT of the EXAFS data can give information on the position of support oxygens and cations with respect to the vanadium atom, as well as on the presence and position of additional vanadium atoms as the vanadium oxide loading increases. Since the number of independent parameters is not infinite, a structural model was used as auxiliary in the fitting procedure. The monomeric model for 1V-Al has been discussed extensively in a previous paper and has been the starting point for the higher loaded catalyst models.[32] The 5V-Al sample reaches 91.8 % of the monomeric monolayer. Presumably, the majority of the vanadium oxide species is still present in monomeric form. This was supported by the large V---$V_{(7)}$ distance (3.5 Å) obtained from EXAFS. Since the V-$O_{(2)}$ distance

is still only 1.71 Å, even a linear V-O-V bond can not have the 3.5 Å V---V distance as a result. The V---$Al_{(5)}$ distance is only slightly different from the 1V-Al sample: 3.07 Å instead of 3.09 Å. The 2.3 Å V---$O_{(4)}$ distance from the alumina support, also observed in the 1V-Al sample, suggest that the anchoring of the vanadium oxide clusters in the 5V-Al sample is the same as in the 1V-Al sample. This is very well possible, since the alumina surface consists of alternating rows of aluminium and oxygen atoms[30-32] and the above mentioned V---Al, V---V and V---$O_{(4)}$ distances can be explained by placing vanadium oxide monomers on adjacent aluminium atoms in the aluminium row. However, two more V---O distances had to be included to complete the fit for the 5 wt% sample. The oxygen contributions at 2.1 Å and 2.91 Å can be ascribed to the oxygen atoms belonging to the neighbouring VO_4 cluster.

The rather large differences in E_0 values for different oxygen shell can be explained by the fact that not all oxygen atoms surrounding the vanadium atom are of the same type. Some are directly connected to the central vanadium atom via a chemical bond (single or double bond), others belong to the supporting oxide or even to a neighbouring VO_4 unit. For each of these different atoms/backscatterers the energy at which a photo-electron can be released (related to the E_0 values in the tables) is different. This results in relatively large dispersion of the ΔE_0 values for the different V-O contributions, especially since all oxygen containing shells were fitted with the same V-O reference made with FEFF 8.

Obviously the 10V-Al and 20V-Al samples have exceeded the monomeric monolayer plentifully. Consequently, the formation of dimeric and/or polymeric vanadium oxide species have to be formed: *i.e.* the V---V has to be short enough to enable a V-O-V bond with V-O distances of 1.71 Å. From the EXAFS a V---V distance of 2.95 Å was observed, and the structural model indicated that this distance was viable for a V-O-V bond. The larger V---O distance of 2.6Å instead of 2.3 Å suggested that the vanadium cluster, more precise the V-O-Al bond, was positioned slightly more parallel to the aluminium row. Furthermore the V---O contributions from the adjacent vanadium cluster were not observed anymore, since the new arrangement of the cluster resulted in much larger distances for these atoms. This explains the large differences in FT between the 5V-Al and the higher loaded samples, as illustrated in Figures A6 and A7.

The increase in pre-edge intensity with increasing loading suggest that the vanadium oxide clusters are changing into more regular tetrahedrons. The formation of a more regular structure is supported by the steady decrease in the Debye-Waller factor for the V-$O_{(2)}$ shell.

Summarizing, when the loading increases the V---V coordination increases as well. Firstly, the surface is filled with monomeric species causing the appearance of a V---V coordination at larger distance, without enabling a V-O-V bond. When the

loading increases vanadium oxide clusters are forced closer together, resulting in the formation of dimeric and polymeric species. Consequently the V---V distance shortened, enabling the V-O-V bond, and the V---V coordination number increases as well.